energies

MDPI

Article

A Full-Controlled Bidirectional Dual-Stage Interleaved Converter for Interfacing AC and DC Power Grids

Goncalo Marques, Vitor Monteiro * and Joao L. Afonso

ALGORITMI Research Centre, LASI, University of Minho, 4800-058 Guimarães, Portugal; pg47215@alunos.uminho.pt (G.M.); jla@dei.uminho.pt (J.L.A.)
* Correspondence: vmonteiro@dei.uminho.pt

Abstract: Power grids are progressing, and the possibility of incorporating DC grids toward hybrid AC/DC grids is gaining increasing relevance, as several technologies available nowadays are operating natively in DC. This paper proposes a topology of a full-controlled bidirectional dual-stage interleaved converter for interfacing hybrid AC/DC grids. The topology is based on a dual-stage architecture, constituted by an AC/DC converter and by a DC/DC converter, both based on interleaved power converters. On the AC side, which is connected to the main AC power grid, the proposed dual-stage architecture operates with sinusoidal current in phase or phase opposition with the voltage, meaning a bidirectional operation. In addition, it has the possibility of interfacing with other AC loads, such as domestic electrical appliances, or with an AC microgrid. The DC link, formed by the AC/DC power stage, is interfaced with a DC power grid, which provides numerous advantages, e.g., for interfacing battery electric vehicles directly charged in DC, as well as other DC loads, such as renewable energy sources. The DC/DC power stage is considered for interfacing with an energy storage system, which is capable of bidirectional power exchange with the DC grid or with the AC grid through the AC/DC power stage. A complete laboratory prototype was designed and developed, with the unified control algorithms implemented on a digital signal processor. The experimental results validated the operation of the full-controlled bidirectional dual-stage interleaved converter based on the specifications for the hybrid AC/DC grid, such as bidirectional operation, synchronization with the AC power grid, predictive current control, interleaved operation on both AC/DC and DC/DC power stages, DC-link voltage control for the DC grid, as well as the operation with different power levels.

Keywords: full-controlled converter; AC and DC power grids; dual-stage interleaved converter; electric mobility; energy storage system

Citation: Marques, G.; Monteiro, V.; Afonso, J.L. A Full-Controlled Bidirectional Dual-Stage Interleaved Converter for Interfacing AC and DC Power Grids. *Energies* **2024**, *17*, 3169. https://doi.org/10.3390/en17133169

Academic Editor: Miguel Castilla

Received: 18 May 2024
Revised: 19 June 2024
Accepted: 24 June 2024
Published: 27 June 2024

1. Introduction

Nowadays, urban mobility worldwide relies heavily on fossil fuels, compromising the sustainability of planet Earth in the medium-to-long term. Despite the continued high pace of fossil fuel exploration in recent years, several countries have made efforts to decarbonize the planet, adopting more sustainable and efficient solutions, such as generating electric power from renewable energy sources [1,2]. The closure of power plants fueled by fossil fuels and the investment in electric mobility, which is intended to, in the long term, replace the current mobility model mostly dependent on fossil fuels, are measures that have been globally adopted [3,4].

Over the past few decades, the increase in the production and utilization of electric vehicles in several contexts has contributed to the recognition of electric mobility as the basis of a new sustainable paradigm that enables socioeconomic development for all countries and benefits future generations. The emergence of electric vehicles has brought significant advantages over traditional internal combustion engine vehicles. For instance, the US Department of Energy launched a project for free domestic electric vehicle charging stations

to raise awareness among the population about electric vehicles [5], and in China, electric mobility has been established as one of the seven emerging strategic industries [6]. Despite these types of indispensable initiatives, it is recognized that the main obstacles to the mass expansion of electric vehicles are universal, such as their high acquisition cost and limited availability of charging points [7]. In addition, the rapid increase in EV adoption is dependent on the development of other technologies and innovative operation modes [8], with special emphasis on electric vehicle chargers (e.g., to allow faster and more efficient charging) and storage technologies (e.g., to allow storing more energy, while increasing the energy density, and to achieve faster charging times) [9]. A review concerning electric vehicle charging technologies, standards, architectures, and power electronics converters is presented in [10].

To manage the electric vehicle charging with off-board chargers, i.e., charging the battery directly in DC, the necessary power can be provided directly from the main power grid (through a three-phase AC/DC power converter) or provided by an external energy storage system (through an DC/DC power converter). The possibility of using an external storage system is an interesting solution for minimizing the impact caused on the main AC power grid since during fast charging high power is required in short periods (e.g., 100 kW in 30 min). In fact, the relevance of using external storage systems (also associated with the interface of renewables) as a complement to DC battery chargers is important, where the emergence of enhanced energy storage systems has proven to be fundamental for the sustained growth of electric mobility in recent decades [11–13]. On the other hand, with the increasing emphasis on renewable energies to reduce carbon dioxide emissions into the atmosphere, external energy storage systems, installed near such power production from renewables, have become essential to balance periods of high and low energy production [14,15]. Based on this, strategic control algorithms can be defined for the power optimization of all parts, namely, the main AC power grid, electric vehicle charging systems, energy storage systems, and power production from renewables.

When analyzing the previous points regarding the interface and native operation of the mentioned technologies, the possibility of hybrid AC/DC grids arises, since EV off-board charging and energy storage systems both operate in DC. Thus, from this point of view, a topology of a full-controlled bidirectional converter for interfacing an AC and a DC power grid is proposed in this paper, which is based on a dual-stage architecture supported by AC/DC and DC/DC interleaved power converters. In this context, a disruptive vision of future power grids supported by hybrid AC and DC power grids is reviewed in [16]. In addition, particularly, a contextualization of smart homes with hybrid AC and DC power grids concerning the role and innovative operation of the front-end AC/DC power converters is analyzed and experimentally verified in [17]. On the other hand, studies concerning power quality in AC and DC power grids are presented in [18], while studies to accomplish power optimization between renewables, energy storage and load shift systems, as well as other technologies, and also permitting energy price management, are presented in [19,20].

From the perspective of implementing previous solutions for hybrid AC/DC grids, the core is centered on power electronics solutions, which are common for all the technologies. Aiming to implement DC grids, AC/DC power electronics converters are required, where typically a two-stage bidirectional structure is necessary based on a front-end converter (i.e., an AC/DC to interface the power grid) and on a back-end (i.e., a DC/DC to interface the DC grid). From this assessment, the main contributions of this paper are summarized as follows: (i) power electronics solution for hybrid AC/DC grids based on full-controlled bidirectional dual-stage interleaved converter with bidirectional operation, allowing the AC grid to supply power to loads connected to the DC grid, including an electric vehicle, other DC native operation loads, as well as an energy storage system, in this case, through a dedicated DC/DC converter; (ii) a bidirectional AC/DC interleaved power converter used as intermediary between the main AC grid and the DC grid, controlling the AC current (i.e., with a sinusoidal waveform and unitary power factor, for improving power quality)

with a predictive current control algorithm and controlling the DC voltage on the DC grid; (iii) a bidirectional DC/DC interleaved power converter used as an intermediary between the DC grid and an energy storage system, which is necessary due to the difference in the voltage levels; (iv) the electric vehicle is directly connected to the DC grid, since the DC/DC conversion is performed on-board the electric vehicle, and, therefore, it can be charged with power from the main AC power grid (through the bidirectional AC/DC interleaved converter) or directly from the energy storage system (through the bidirectional DC/DC interleaved converter); (v) possibility of reverse operation, with the electric vehicle providing power to the AC grid or to the storage system, offering a set of power control possibilities for both AC and DC grids; and (vi) experimental validation supported by a power electronics prototype, including power systems and digital control, completely developed for the purpose of this paper. An experimental validation of a similar topology is presented in [21] to integrated electric vehicles and renewables, but without any energy storage systems, such as is proposed in this paper. A study about the contextualization of hybrid AC/DC power grids to support the integration of electric vehicles, renewables, and energy storage is presented in [22], but the detail of the power converters is not introduced, as proposed in this paper.

The proposed architecture of the full-controlled bidirectional dual-stage interleaved converter for interfacing AC and DC power grids, as presented in Figure 1, is discussed in Section 2, while the respective control algorithms are described in Section 3, which are corroborated by the experimental validation presented in Section 4. Conclusions are given in Section 5.

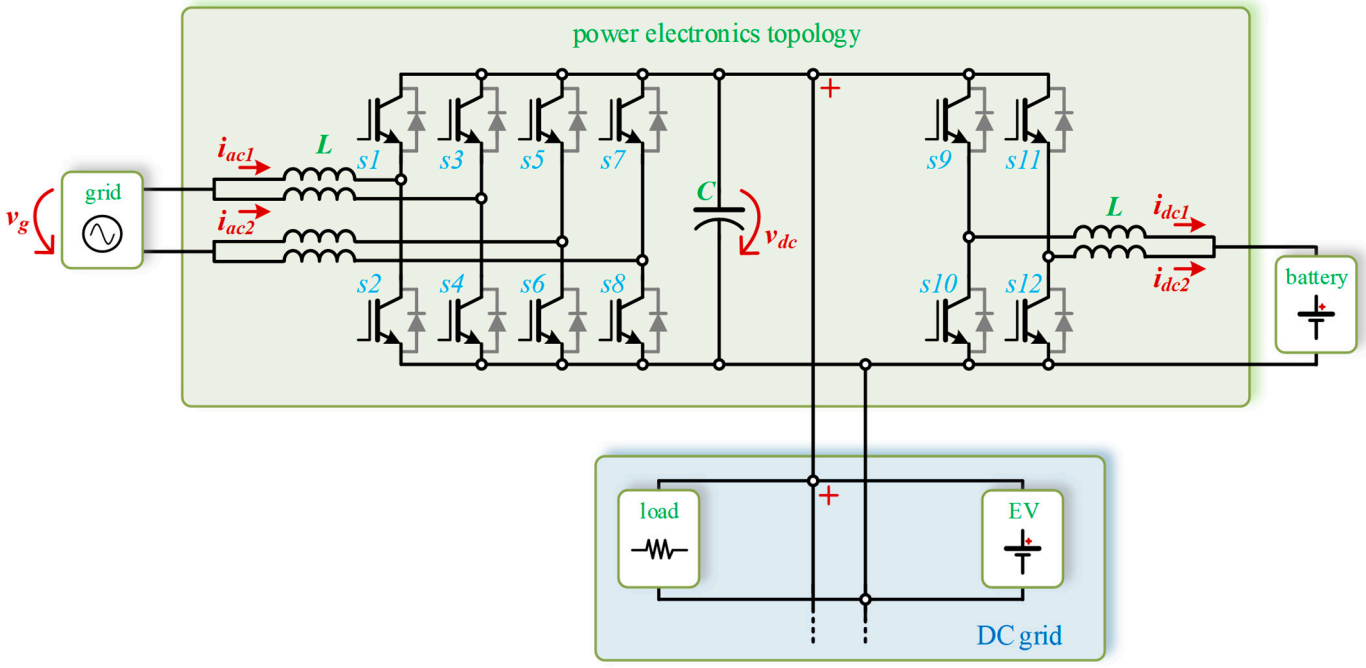

Figure 1. Power electronics topology of the proposed full-controlled bidirectional dual-stage interleaved converter for interfacing AC and DC power grids.

2. Topology of the Full-Controlled Bidirectional Dual-Stage Interleaved Converter

The topology of the full-controlled bidirectional dual-stage interleaved converter is based on an AC/DC and a DC/DC converter, where the interleaved AC/DC allows interleaving n arms in parallel [23], and where the currents in each arm are controlled with a fixed switching frequency, whose ripples are phase-shifted (ϕ) according to

$$Ø = 360^{\circ}/n. \quad (1)$$

The AC/DC topology consists of eight power semiconductors and offers several advantages over the traditional full-bridge topology. It reduces the value of the current produced by each arm, leading to decreased losses, and a significant reduction in total harmonic distortion (THD). In addition, as a key feature of such topology, it also almost eliminates the ripple in the converter's output current [24,25] (this situation of eliminating the ripple just occurs when the duty-cycle is 50%). However, this topology also has some disadvantages, such as the use of a larger number of coupling inductors with the AC grid (even considering that the nominal current is lower), as well as a higher number of driver circuits and signal conditioning channels for the voltage and current sensors, contributing to a less compact converter. Like the full-bridge converter, also an important feature, this converter can generate three levels of voltage at its output, namely, $+vdc$, zero, and $-vdc$. Similarly, the DC/DC converter is also based on an interleaved structure, offering more advantages compared to other conventional topologies, such as a traditional half-bridge DC/DC converter. Therefore, over the years, it has been used more frequently in power electronics systems [25,26]. Analyzing the main advantages of this converter, a significant reduction in conduction losses in IGBTs stands out, as the current is divided by the two arms, reducing its nominal value by half. In addition, as an advantage, this converter also can continue its operation in case one of the IGBTs becomes inoperable, which is not the case with traditional topologies (this is a possibility, but in such circumstances, necessarily it will operate with reduced power, which can be preferable than a complete turn-off). The main disadvantages of this topology are related to the higher number of power semiconductors (and consequently the number of gate drivers and sensors, for instance), leading to higher costs and greater complexity in its design, implementation, and control [26,27]. Despite these disadvantages, this topology proves to be the most efficient and reliable choice for integration into a system that enables the interface of native DC technologies (e.g., DC power grids and systems of battery charging and energy storage).

The full-controlled bidirectional dual-stage interleaved converter, illustrated in Figure 1, allows the complementation of the functionalities offered by each interleaved converter in a unique solution. Tables 1 and 2 show the different operating states of the IGBTs, respectively, for the AC/DC and DC/DC power converters, when operating in bidirectional mode, where v_{conv} means the voltage between the switching devices and the coupling filters; i.e., it is the voltage produced by the converter, where it is possible to verify the distinct levels.

Table 1. Operating states of the interleaved AC/DC converter.

v_g	s1	s2	s3	s4	s5	s6	s7	s8	$v_{conv\,\{1,2\}}$
Positive half-cycle	ON	OFF	OFF	ON	OFF	ON	ON	OFF	$+v_{dc}$
	ON	OFF	ON	OFF	OFF	ON	OFF	ON	0
	OFF	ON	OFF	ON	ON	OFF	ON	OFF	0
	OFF	ON	ON	OFF	ON	OFF	OFF	ON	$-v_{dc}$
Negative half-cycle	OFF	ON	ON	OFF	ON	OFF	OFF	ON	$+v_{dc}$
	OFF	ON	OFF	ON	ON	OFF	ON	OFF	0
	ON	OFF	ON	OFF	OFF	ON	OFF	ON	0
	ON	OFF	OFF	ON	OFF	ON	ON	OFF	$-v_{dc}$

Table 2. Operating states of the interleaved DC/DC converter.

Operation Modes	s9	s10	s11	s12	$v_{conv\ \{1,2\}}$
Boost	ON	OFF	OFF	ON	$+v_{dc}$
	ON	OFF	ON	OFF	0
	OFF	ON	OFF	ON	0
	OFF	ON	ON	OFF	$-v_{dc}$
Buck	OFF	OFF	ON	ON	$+v_{dc}$
	ON	OFF	OFF	ON	0
	OFF	ON	ON	OFF	0
	ON	ON	OFF	OFF	$-v_{dc}$

3. Control Algorithms of the Full-Controlled Bidirectional Dual-Stage Interleaved Converter

The application of digital current control techniques in power electronics converters constitutes one of the most important steps in implementing these systems. In the architecture of the power electronics topology proposed in this paper, the application of a suitable digital control technique enables better results to be achieved, particularly with the objective of reducing the AC and DC current ripple.

3.1. Current Control of AC/DC Converter

Regarding the AC/DC converter, the applied digital current control is supported by a predictive current control technique, which is based on the electrical model of the system, and generates the reference voltage ($v_{conv\ \{1,2\}}$) for comparison with the carriers that generate the gate control signals for the IGBTs (i.e., the implementation of the pulse-width modulation). Therefore, with this predictive current control technique, combined with a modulator, it is possible to achieve controlled variables with fixed frequency (f_{sw}). For such purpose, it is necessary to know the values of certain variables and parameters that are part of the system as the reference current (i_{ref}), which is obtained based on the acquired voltage and current in the AC grid (v_{grid}) and its RMS values, and the value of grid coupling inductance (L), as well as the operating power on the DC side, where the DC/DC converter and the other DC native operating technologies are connected (e.g., the electric vehicle). The calculation of the reference voltage ($v_{conv\ \{1,2\}}$) is performed in the prediction model [28,29]:

$$v_{conv\{1,2\}} = v_{grid} - \left[f_{sw}\ L \left(i_{ref} - i_g \right) \right]. \quad (2)$$

This technique has several advantages, notably the fact that it does not require adjusting control action parameters, unlike PI control, promoting a fast and much more stable response. The main drawback of this control technique is its high sensitivity to electromagnetic interference in the measurement of voltage and current values, which can cause errors in the calculation of the reference voltage [29,30].

3.2. Current Control of DC/DC Converter

The PI current control technique is a control method that calculates the error between the reference current and the current produced by the converter and implements an integral over such error, also establishing the respective proportional integral gain. The output result of the PI control is compared to a fixed-frequency triangular carrier waveform to synthesize the PWM control signals that enable the switching of power semiconductors of the DC/DC converter. Figure 2 shows a representative block diagram of a PI controller, which was used to control the voltage of the DC link and the output voltage and current of the DC/DC converter.

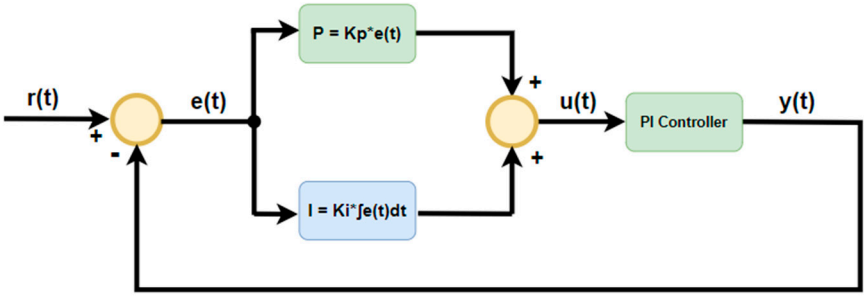

Figure 2. Representative block diagram of a PI controller, which was used to control the voltage of the DC link and the output voltage and current of the DC/DC converter.

The variable $e(t)$ represents the error, i.e., it is equal to the difference between the desired value for the output $r(t)$ and the actual measured value $y(t)$. The control signal $u(t)$ is obtained by summing the two components: one proportional to the error and the other proportional to the integral of the error. The constant Kp defines the proportional gain, and Ki makes it possible to adjust the integral gain. However, the main disadvantages of this control lie in the need to adjust the proportional and integral gains, resulting in oscillations in the system's behavior [31].

3.3. SPWM Modulation

The bipolar sinusoidal pulse width modulation (SPWM) technique involves comparing a sinusoidal reference ($v_{conv\ \{1,2\}}$) with a triangular carrier wave (v_{tri}). From this comparison, the control signals for switching the IGBTs are obtained. In this process, as there is only a single comparison, it is only possible to generate two voltage levels, $+vdc$ and $-vdc$ [32]. In contrast to bipolar modulation, unipolar SPWM modulation involves another reference wave. This wave differs from the first one, as it has a phase shift of 180°. To perform this modulation technique, an additional comparator is required. In addition, through this process, it is possible to obtain three voltage levels at the converter's output: $+vdc$, 0, and $-vdc$. This modulation technique has several advantages over bipolar SPWM modulation, such as allowing the IGBTs to switch at a frequency that is double the switching frequency for bipolar modulation, and to reduce the voltage across the coupling filter, which means the possibility of reducing its value for the same amplitude of the current ripple.

4. Developed Prototype and Laboratory Experimental Validation

This section introduces the laboratory prototype, specifically developed in the scope of this paper, and the obtained experimental results. The key parameters used in the design of the full-controlled bidirectional dual-stage interleaved converter are presented in Table 3. As presented, the RMS value of the AC grid voltage is 230 V, and the DC-link voltage is 400 V; i.e., a value greater than the maximum instantaneous voltage of the power grid voltage. The battery voltage value is below the power grid voltage since the interleaved DC/DC power converter is used for this purpose (operating as a step-down converter, in buck mode, reducing the DC-link voltage to the battery voltage). When the battery is charging, the interleaved DC/DC converter operates in buck mode, while when the battery is discharging, the interleaved DC/DC converter operates as a step-up converter, in boost mode. The same reasoning is applied to the AC/DC converter, which is controlled by current in the interface with the AC power grid. The AC/DC power converter operates with a control algorithm based on an outer control loop for controlling the DC-link voltage, and based on an inner control loop for controlling the AC current (ensuring sinusoidal current in phase or in phase opposition with the AC power grid voltage, depending on the operation as active rectifier or grid-tied inverter).

Table 3. Design parameters of the full-controlled bidirectional dual-stage interleaved converter.

Parameters	Value	Unit
Power Grid Nominal Voltage	230	V
DC-Link Nominal Voltage	400	V
Battery Nominal Voltage	100–400	V
Power Grid Nominal Current	16	A
Battery Nominal Current	10	A
Power Grid Nominal Power	3.68	W
Coupling Inductors (Battery Side)	2.5	mH
Coupling Inductors (Power Grid Side)	5	mH
Coupling Capacitors (DC-Link)	1.5	mF
Power Grid Voltage Frequency	50	Hz
Sampling Frequency	40	kHz
Switching Frequency	20	kHz

The design of the laboratory prototype is also presented in this section, highlighting the main features and the components used. It is a laboratory prototype, but it was designed to be considered as a pre-industrial prototype, where the main circuits (e.g., sensors, signal conditioning, and gate drivers) are on the same board, representing an attractive approach aligned with a perspective of industrialization. The developed prototype of the full-controlled bidirectional dual-stage interleaved converter is presented in Figure 3, where the main parts are highlighted. The IGBTs are soldered on this board, but the package is positioned on the bottom side, allowing a direct connection with the heatsink.

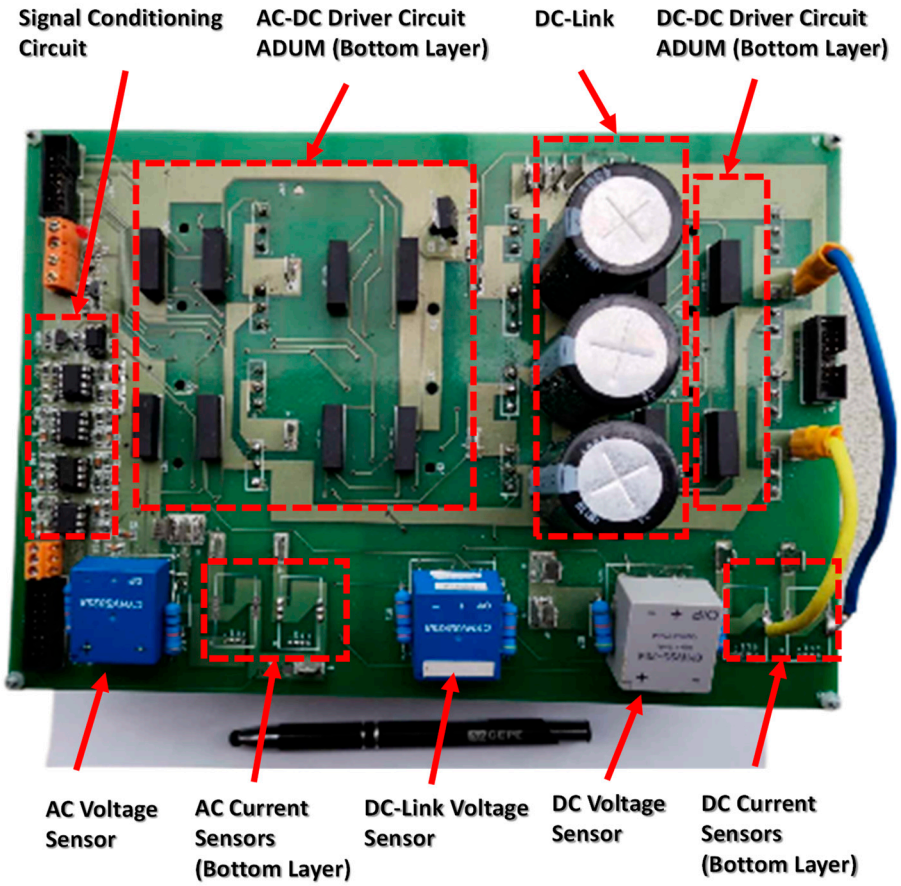

Figure 3. Developed prototype of the full-controlled bidirectional dual-stage interleaved converter.

In terms of objectives of the experimental validation, the results were obtained in different conditions, including individual validation of the power converters, and inte-

grated validation, with both AC/DC and DC/DC converters working together, regulating the voltages and currents in the distinct interfaces. For the AC/DC converter, the key features were validated: operation in interleaved mode; operation with controlled output DC voltage; synchronization with the power grid AC voltage using a phase-locked loop (PLL); validation of the produced voltages with three levels; and validation in bidirectional mode. For the DC/DC converter, the operation was validated mainly in interleaved mode. A complete description and discussion concerning the experimental validation is presented in this section, corroborating the proposal of this paper.

4.1. Developed Prototype

To obtain the experimental results validating the operation of the full-controlled bidirectional dual-stage interleaved converter, the prototype depicted in Figure 3 was developed and tested in the laboratory, under real operating conditions, and directly connected to the power grid AC voltage, avoiding the necessity of any controlled AC power supply. The control circuit consists of the signal conditioning circuit for interfacing the output signals from the voltage and current sensors, individually isolated gate-drivers circuits for the IGBTs, and a digital signal processor (DSP) TMS320F28335 by Texas Instruments for the digital control implementation. The signal acquisition for voltage and current was performed at a sampling frequency of 40 kHz, while the switching frequency for the IGBTs was fixed with a value of 20 kHz, using the implemented current control and modulation techniques. The used voltage and current sensors are based on hall-effect sensors, CYHVS5-25 and LTSR 15-NP, respectively. The selected IGBTs have the reference HW30N120R5. The coupling inductors have an inductance of 3 mH with a nominal current of 20 A. A capacitor with a capacity of 1680 µF is used in the created DC grid, which allows withstanding of a maximum voltage of 400 V. Figure 4 shows the laboratory setup that was prepared to obtain experimental results, with a focus on the full-controlled interleaved converter, and the digital oscilloscope Yokogawa DL708E.

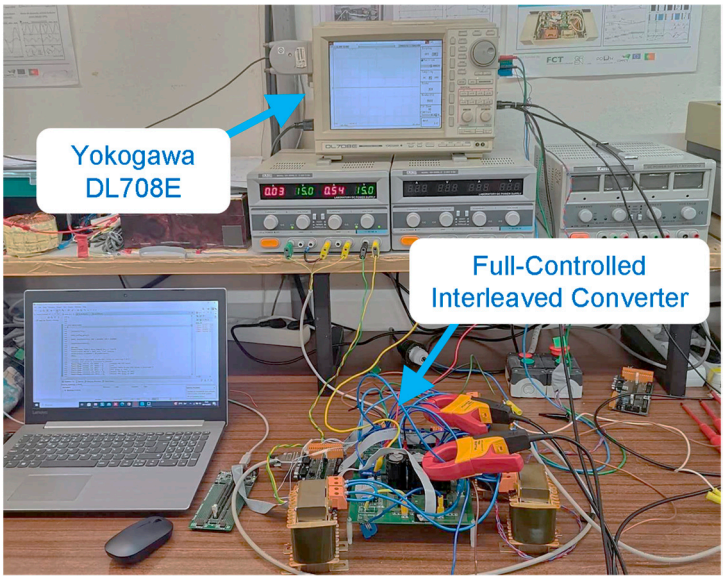

Figure 4. Laboratory setup prepared to obtain the experimental results.

4.2. Experimental Results

Regarding the DC/DC converter, the experimental validation aimed to thoroughly assess the operational integrity of the developed interleaved DC/DC converter under closed-loop conditions. A meticulous examination of current profiles in both buck and boost modes was undertaken to validate the converter's performance. The currents in these modes were meticulously analyzed as they represent the cumulative currents flowing through each arm of the converter. Of particular interest was the scrutiny of the current

ripple and the phase relationship between the currents, which are distinctive features of interleaved converters and are essential for their optimal operation. In the validation test for current control in buck mode, a precisely controlled 40 V voltage was supplied by a DC source at the DC link. A resistive load of 26 Ω was considered and connected to simulate practical operating conditions, in order to validate the PI current control technique for a reference current of 1 A. Figure 5 illustrates the currents flowing through each arm of the converter, capturing the intricate 40 kHz ripple and the precisely maintained 180° phase shift between them. These observations validate the effectiveness of the current control technique, confirming its capability to regulate the converter's operation in buck mode with high fidelity. Similarly, the validation of the DC/DC converter's operation in boost mode involved meticulous testing. The PI current control technique was judiciously applied to ensure precise regulation of the output current. In this scenario, a 40 V DC source was again employed, this time with a 13 Ω resistor connected on the DC-link side to simulate the reverse process according to previously defined load conditions. Figure 6 shows the currents in each arm of the converter, highlighting the consistent 40 kHz ripple and the precisely maintained 180° phase shift. These results unequivocally demonstrate the converter's proficiency in boost-mode operation and underscore the robustness of the applied control strategy.

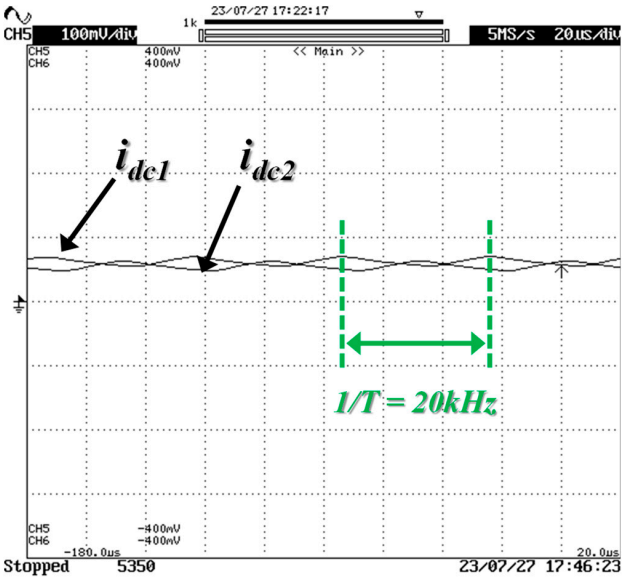

Figure 5. Currents in each arm of the interleaved DC/DC converter, for a reference current of 1 A with PI current control, in buck mode.

Transitioning to a broader scope, the experimental validation expanded to encompass the interleaved AC/DC converter's functionality both as an active rectifier and grid-tied inverter. The initial phase of experimentation focused on assessing the converter's efficacy as an active rectifier, emphasizing the seamless operation of the implemented Sinusoidal Pulse Width Modulation (SPWM) technique, precisely synchronized with the AC power grid. Furthermore, meticulous attention was paid to the efficacy of the current control strategy and the stability of the voltage regulation on the DC link. Subsequently, the evaluation extended to assess the converter's performance as a grid-tied inverter. The focus shifted toward evaluating the converter's capability to inject power into the AC power grid across varying power levels. This comprehensive analysis provided invaluable insights into the converter's suitability for bidirectional power flow applications, affirming its versatility and robustness across diverse operational scenarios.

The modulation technique employed to regulate the IGBTs of the interleaved AC/DC converter is the unipolar SPWM technique. Figure 7 provides a detailed depiction of the PWM signals controlling the IGBTs labeled "PWM3B_AT" and "PWM3A_AB", which

pertain to the first h-bridge of the AC/DC converter. Notably, the implementation of dead-time is evident in the figure, effectively preventing the simultaneous activation of IGBTs within the same arm. This ensures safe and efficient switching operation, mitigating the risk of shoot-through currents, and enhancing the converter's reliability. Furthermore, Figure 8 elucidates the voltage waveforms generated by the interleaved AC/DC converter, confirming the precise operation of the unipolar SPWM modulation technique at a switching frequency of 20 kHz. These voltage waveforms validate the effective switching of the IGBTs, showcasing the desired three voltage levels required for the proposed operation of the AC/DC conversion. To validate the synchronization technique with the AC grid, the integration with the power grid was facilitated through a 230 V:25 V transformer. Figure 9 presents a comprehensive view of the power grid voltage alongside the output signal generated by the enhanced PLL (ePLL). Notably, this figure captures the crucial moment when the ePLL voltage achieves complete synchronization with the AC power grid voltage in terms of amplitude, phase, and frequency. This synchronization is crucial for ensuring a seamless integration of the interleaved AC/DC converter with the power grid, facilitating the efficient and reliable power transfer between the converter and the AC power grid.

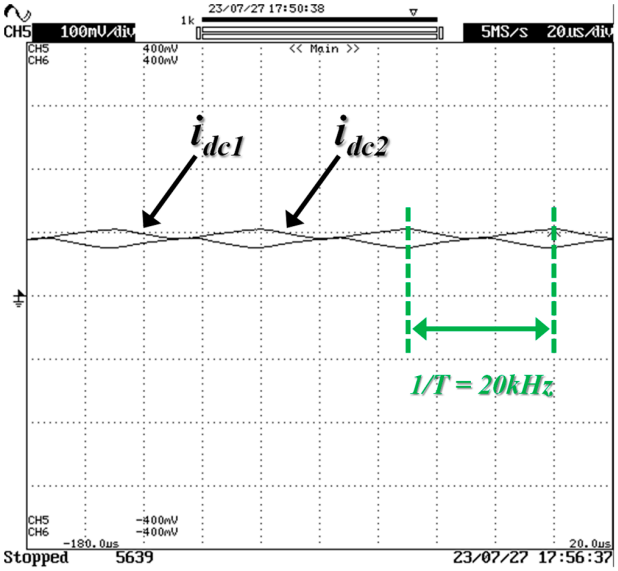

Figure 6. Currents in each arm of the interleaved DC/DC converter, for a reference current of 2 A with PI current control, in boost mode.

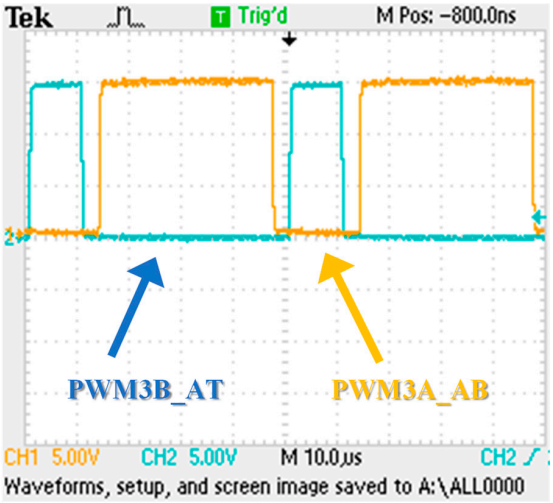

Figure 7. PWM3B_AT signals (CH1) and the PWM signal PWM3A_AB (CH2), with dead-time application.

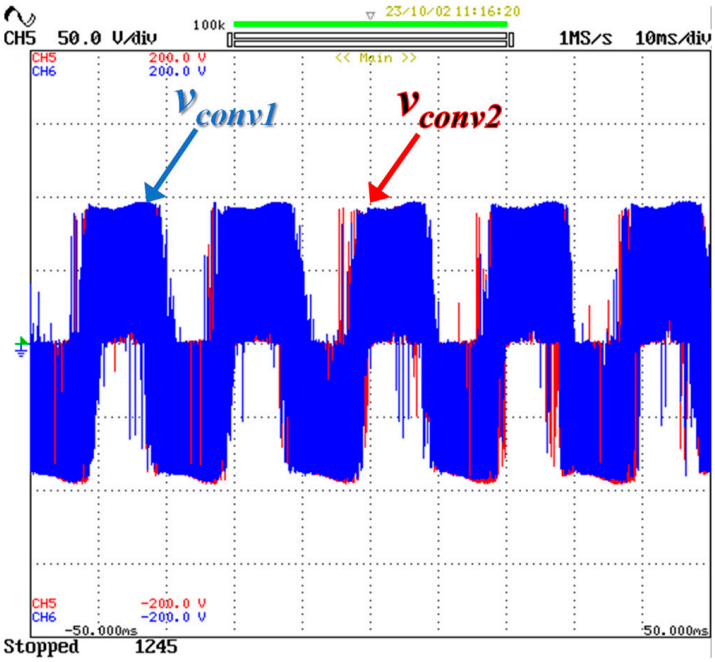

Figure 8. Three voltage levels produced by the interleaved AC/DC converter.

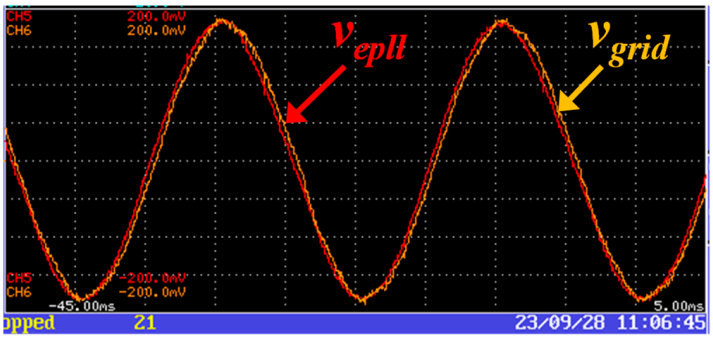

Figure 9. Synchronization of the generated ePLL voltage with the power grid voltage.

The validation of the implemented predictive current control technique, crucial for regulating the currents drawn by the AC/DC converter, involved the utilization of a transformer with a voltage ratio of 230 V:50 V and a DC-link voltage of 70 V. Through the application of the predictive current control technique with a predefined reference current of 5 A, an effective current of 5 A was achieved. This effective current is derived from the summation of the individual currents produced by the AC/DC converter, each attaining an effective value of 2.5 A, as illustrated in Figure 10, which underscores the reliability of the implemented control strategy. Furthermore, the ripple characteristics and the phase relationship between the currents are comprehensively depicted in Figure 11. Notably, the presence of ripple in each current waveform is observed, which is indicative of the dynamic nature of the AC/DC converter operation. Additionally, the consistent 180° phase shift between the individual currents underscores the interleaved nature of the AC/DC converter, confirming its inherent capability for power conversion.

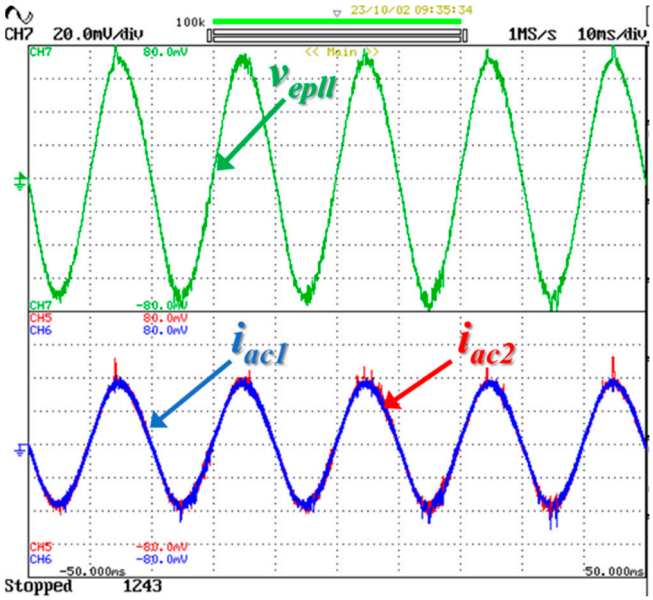

Figure 10. Operation of the interleaved AC/DC converter as an active rectifier, after applying the predictive current control technique for a reference current of 5 A, with an operating power of 125 W.

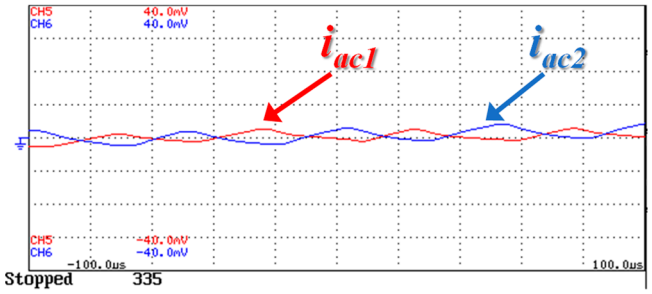

Figure 11. Ripple present in the currents produced by the interleaved AC/DC converter, with a phase-shift of 180°, for a reference current of 5 A.

After the successful validation of the current control technique, the focus shifted toward validating the control of the voltage on the DC link. This process involved the utilization of the PI control technique, comparing the measured DC-link voltage with a predefined reference voltage. Effective management of the DC-link voltage via the PI control mechanism enables precise adjustment of the reference current, thereby facilitating control over the operational power of the interleaved AC/DC converter. In this validation test, an AC RMS voltage of 50 V was applied, stabilizing the voltage on the DC link at 100 V. Consequently, a current with an effective value of 7 A was obtained, resulting in the converter operating at a power output of 350 W. Figure 12 visually depicts the controlled voltage on the DC link at 100 V alongside the currents consumed by the converter, each with an RMS value of 3.5 A (i.e., a current in each arm). The experimental results unequivocally confirm the successful implementation of the voltage control on the DC link, validating the operational integrity of the control strategy. Following the validation of the interleaved AC/DC converter's operation as an active rectifier, it was imperative to validate its functionality also as a grid-tied inverter. This validation test involved applying a 50 V RMS voltage from the AC power grid, while maintaining a voltage of 100 V on the DC link. Leveraging the predictive current control technique, a reference current of 3.5 A was generated, enabling the interleaved AC/DC converter to inject a corresponding current of 3.5 A into the AC grid, operating at a power output of 175 W. Figure 13 illustrates the phase relationship between the voltage from the AC power grid and the currents produced by the converter, confirming its seamless operation as an inverter. Finally, a transient-state test

was conducted to evaluate the interleaved AC/DC converter's performance, operating as an inverter under varying values of power. This test involved applying different reference currents of 2 A and 4 A. Initially, a reference current of 2 A was applied, resulting in the converter operating at a power output of 100 W, and injecting a corresponding current of 2 A into the AC power grid. Upon transitioning to the next state, the reference current doubled to 4 A, leading to a proportional increase in the injected current and operating power, which rose to 200 W. Figure 14 presents the obtained results, validating the interleaved AC/DC converter's capability to operate as an inverter, injecting energy into the AC grid across different operating power levels.

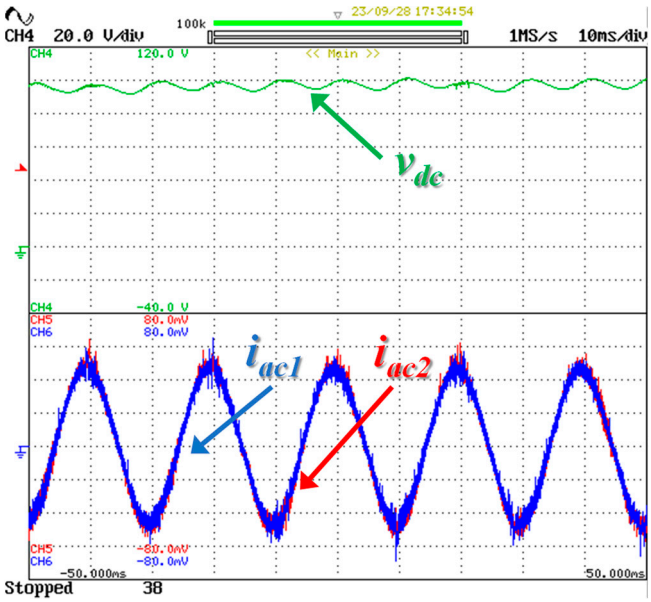

Figure 12. Control of the DC-link voltage to a value of 100 V; currents consumed by the interleaved AC/DC converter for a reference current of 7 A, with an operating power of 350 W.

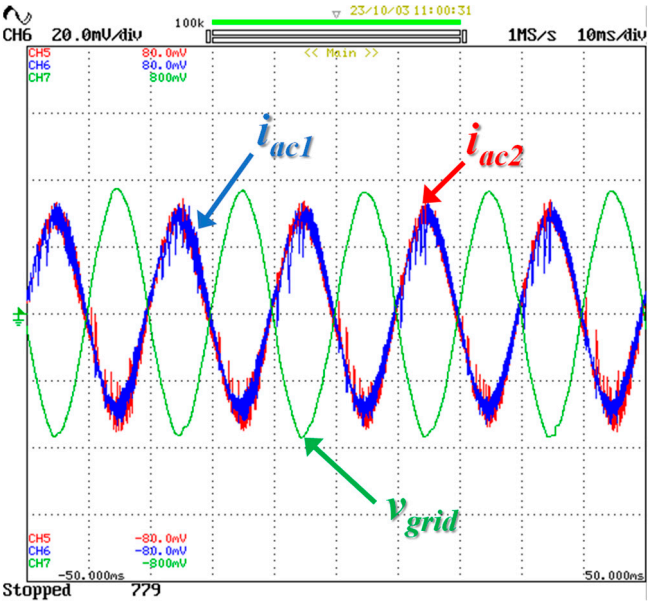

Figure 13. Operation of the interleaved AC/DC converter as an inverter, injecting a current of 3.5 A into the power grid, with an operating power of 175 W.

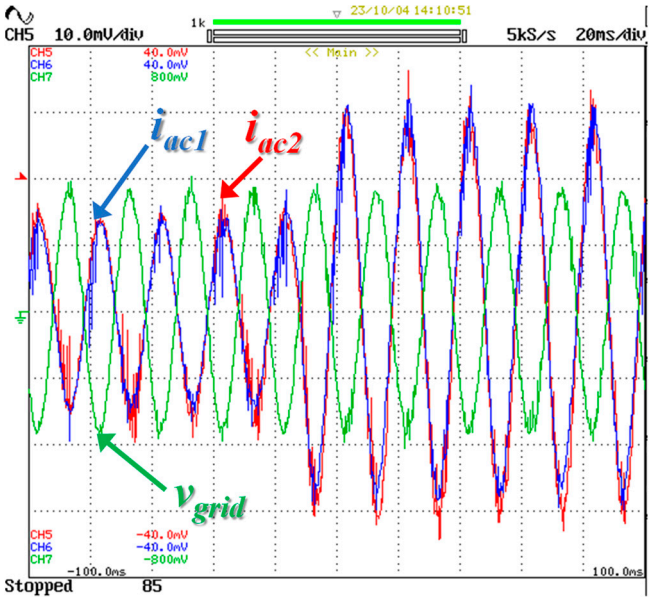

Figure 14. Operation of the interleaved AC/DC converter as an inverter, for an operating power of 100 W at a reference current of 2 A and an operating power of 200 W at a reference current of 4 A.

5. Conclusions

Worldwide, the growth in technologies such as electric mobility, energy storage systems, DC power grids, and renewables is changing the energy paradigm toward more sustainable smart grids. In this scope, the main aim of this paper is to contribute with a proposed full-controlled bidirectional dual-stage interleaved topology, where the implemented current control and modulation techniques, specifically predictive and PI current control techniques, as well as bipolar and unipolar PWM techniques, are detailed. The design for both the AC/DC and DC/DC power stages of the prototype is presented, emphasizing the components and the different circuits composing the control and power stages. The experimental validation in a steady and transient state was obtained in different conditions, including the individual validation of the power converters and the integrated validation, highlighting the effectiveness of the implemented PLL synchronization technique with the power grid. The current control technique and the DC-link voltage control were shown to work effectively, ensuring robust and stable operation of the converter across various operating power levels, and it is worth noting the converter's performance at a power level of 350 W and a stable DC-link voltage of 100 V, which proves the stability of the current control techniques applied. Finally, noteworthy results were obtained in validating the converter as an inverter, i.e., with the grid voltage and current in phase opposition, returning power back to the power grid. Additionally, the converter demonstrated the ability to inject varying amounts of power into the power grid, depending on changes in the operating power of the interleaved AC/DC converter.

Author Contributions: Methodology, G.M.; validation; investigation, G.M., J.L.A. and V.M.; writing—original draft preparation, G.M.; writing—review and editing, V.M. and J.L.A.; funding acquisition, V.M. and J.L.A. All authors have read and agreed to the published version of the manuscript.

Funding: This research received no external funding.

Data Availability Statement: Data is contained within the article.

Acknowledgments: This work has been supported by the Project "ATE Alinaça para a Transição Energética-Alliance for the Energy Transition" (C644914747-00000023/56).

Conflicts of Interest: The authors declare no conflicts of interest.

References

1. Udaeta, M.; Chaud, C.; Gimenes, A.; Galvao, L. Electric Vehicles Analysis inside Electric Mobility Looking for Energy Efficient and Sustainable Metropolis. *Open J. Energy Effic.* **2015**, *4*, 54339. [CrossRef]
2. Barreto, R.; Faria, P.; Vale, Z. Electric Mobility: An Overview of the Main Aspects Related to the Smart Grid. *Electronics* **2022**, *11*, 1311. [CrossRef]
3. Murano, V.; Muratori, M.; Rizzo, G.; Rizzoni, G. Electric Mobility: From Fossil Fuels to Renewable Energy, Opportunities and Challenges. *IFAC Proc. Vol.* **2013**, *46*, 812–817.
4. Al-Ghaili, A.; Kazim, H.; Aris, H.; Al-Hada, N. Can electric vehicles be an alternative for traditional fossil-fuel cars with the help of renewable energy sources towards energy sustainability achievement? *Energy Inf. Acad. Conf. Den.* **2022**, *5*, 60. [CrossRef]
5. Lankao, P.; Wilson, A.; Schimtt, D. Inequality and the future of electric mobility in 36 U.S. Cities: An innovative methodology and comparative assessment. *Energy Res. Soc. Sci.* **2022**, *91*, 102760. [CrossRef]
6. Yan, X.; Wang, L.; Chai, Z.; Zhao, S.; Liu, Z.; Sun, X. Electric vehicle battery simulation system for mobile field test of off-board charger. *Energies* **2019**, *14*, 3025. [CrossRef]
7. Ahmad, M.; Pesyridis, A.; Sphicas, P.; Andwari, A.; Gharehghani, A.; Vaglieco, B. Electric Vehicle Modelling for Future Technology and Market Penetration Analysis. *Front. Mech. Eng.* **2022**, *8*, 896547. [CrossRef]
8. Lenka, R.K.; Panda, A.K.; Dash, A.R.; Senapati, L.; Tiwary, N. A Unified Control of Grid-Interactive Off-Board EV Battery Charger With Improved Power Quality. *IEEE Trans. Transp. Electrif.* **2023**, *9*, 920–933. [CrossRef]
9. Hamednia, A.; Murgovski, N.; Fredriksson, J.; Forsman, J.; Pourabdollah, M.; Larsson, V. Optimal Thermal Management, Charging, and Eco-Driving of Battery Electric Vehicles. *IEEE Trans. Veh. Technol.* **2023**, *72*, 7265–7278. [CrossRef]
10. Acharige, S.S.G.; Haque, M.E.; Arif, M.T.; Hosseinzadeh, N.; Hasan, K.N.; Oo, A.M.T. Review of Electric Vehicle Charging Technologies, Standards, Architectures, and Converter Configurations. *IEEE Access* **2023**, *11*, 41218–41255. [CrossRef]
11. Li, N.; Wu, J.; Li, Q.; Hu, J.; Fan, H.; Huang, B. Research on Application and Benefits of Energy Storage Systems. *E3S Web Conf.* **2022**, *338*, 01011. [CrossRef]
12. Faisal, M.; Hannan, M.A.; Ker, P.J.; Hussain, A.; Mansor, M.B.; Blaabjerg, F. Review of energy storage system technologies in microgrid applications: Issues and challenges. *IEEE Access* **2018**, *6*, 35143–35164. [CrossRef]
13. Mitali, J.; Dhinakaran, S.; Mohamad, A. Energy storage systems: A review. *Energy Storage Sav.* **2022**, *1*, 166–216. [CrossRef]
14. Sayed, E.; Olabi, A.; Alami, A.; Radwan, A.; Rezk, A.; Abdelkareem, M. Renewable Energy and Energy Storage Systems. *Energies* **2023**, *16*, 1415. [CrossRef]
15. Tan, K.; Babu, T.; Ramachandaramurthy, V.; Kasinathan, P.; Solanki, S.; Raveendran, S. Empowering smart grid: A comprehensive review of energy storage technology and application with renewable energy integration. *J. Energy Storage* **2021**, *39*, 102591. [CrossRef]
16. Monteiro, V.; Martins, J.S.; Fernandes, A.; Afonso, J.L. Review of a Disruptive Vision of Future Power Grids: A New Path Based on Hybrid AC/DC Grids and Solid-State Transformers. *Sustainability* **2021**, *13*, 9423. [CrossRef]
17. Mohammed, S.A.Q.; Jung, J.-W. A State-of-the-Art Review on Soft-Switching Techniques for DC–DC, DC–AC, AC–DC, and AC–AC Power Converters. *IEEE Trans. Ind. Inform.* **2021**, *17*, 6569–6582. [CrossRef]
18. Bracale, A.; Caramiaa, P.; Carpinelli, G.; Mottola, F.; Proto, D. A Hybrid AC/DC Smart Grid to Improve Power Quality and Reliability. In Proceedings of the 2012 IEEE International Energy Conference and Exhibition (ENERGYCON), Florence, Italy, 9–12 September 2012; pp. 507–514.
19. Vuyyuru, U.; Maiti, S.; Chakraborty, C. Active Power Flow Control Between DC Microgrids. *IEEE Trans. Smart Grid* **2019**, *10*, 5712–5723. [CrossRef]
20. Kinhekar, N.; Padhy, N.P.; Li, F.; Gupta, H.O. Utility Oriented Demand Side Management Using Smart AC and Micro DC Grid Cooperative. *IEEE Trans. Power Syst.* **2016**, *31*, 1151–1160. [CrossRef]
21. Monteiro, V.; Pinto, J.; Afonso, J. Experimental Validation of a Three-Port Integrated Topology to Interface Electric Vehicles and Renewables with the Electrical Grid. *IEEE Trans. Ind. Informa.* **2018**, *14*, 2364–2374. [CrossRef]
22. Gupta, A.; Doolla, S.; Chatterjee, K. Hybrid AC–DC Microgrid: Systematic Evaluation of Control Strategies. *IEEE Trans. Smart Grid* **2018**, *9*, 3830–3843. [CrossRef]
23. Sosa-Zuniga, J.; Rodriguez-Cortes, C.; Martinez-Rodriguez, P.; Vazquez-Guzman, G. Multi-Phase Interleaved AC–DC Step-Down Converter with Power Factor Improvement. *Micromachines* **2023**, *14*, 511. [CrossRef] [PubMed]
24. Seyezhai, R.; Aarthi, V. Simulation and implementation of ac-dc interleaved boost converter with voltage multiplier for phev. *ICTACT J. Microelectron.* **2016**, *2*, 247–253. [CrossRef]
25. Tashakor, N.; Khooban, M.H. An Interleaved Bi-Directional AC-DC Converter with Reduced Switches and Reactive Power Control. *IEEE Trans. Circuits Syst. II Express Briefs* **2020**, *67*, 132–136. [CrossRef]
26. Vellaiyarasi, M.; Esakki, K.; Loga, S.; Jasper, J.; Chandran, G. Interleaved Buck Boost Converter Fed DC Motor. 2013. Available online: http://www.irphouse.com (accessed on 20 June 2024).
27. Gules, R.; Lopes, L.; Luis, P.; Franco, C. An Interleaved Boost Dc-Dc Converter with Large Conversion Ratio. *IEEE Symp. Ind. Electron.* **2003**, *1*, 411–416. [CrossRef]
28. Comarella, B.; Carletti, D.; Yahyaoui, I.; Encarnação, L. Theoretical and Experimental Comparative Analysis of Finite Control Set Model Predictive Control Strategies. *Electronics* **2023**, *12*, 1482. [CrossRef]

29. Vazquez, S.; Rodriguez, J.; Rivera, M.; Franquelo, L.; Norambuena, M. Model Predictive Control for Power Converters and Drives: Advances and Trends. *IEEE Trans. Ind. Electron.* **2017**, *64*, 935–947. [CrossRef]
30. Barrero-González, F.; Milanés-Montero, M.I.; González-Romera, E.; Romero-Cadaval, E.; Roncero-Clemente, C. Control strategy for electric vehicle charging station power converters with active functions. *Energies* **2019**, *12*, 3971. [CrossRef]
31. Pedrosa, D.; Gomes, R.; Monteiro, V.; Fernandes, J.; Monteiro, J.; Afonso, J. Model predictive control of an on-board fast battery charger for electric mobility applications. In *Lecture Notes in Electrical Engineering, Proceedings of the CONTROLO 2016: Proceedings of the 12th Portuguese Conference on Automatic Control, Guimarães, Portugal, 14–16 September 2016*; Springer: Cham, Switzerland, 2017; pp. 679–689. [CrossRef]
32. Holmes, D.G.; Lipo, T. *Pulse Width Modulation for Power Converters: Principles and Practice*; John Wiley: Hoboken, NJ, USA, 2003.